DOI: 10.15849/IJASCA.251130.11

Int. J. Advance Soft Compu. Appl, Vol. 17, No. 3, November 2025
Print ISSN: 2710-1274, Online ISSN: 2074-8523

Numerical Approach to Fractional Model for Dispersion, Dissipation, and Diffusion with a Logistic Reaction

Ilhem KADRI[1*], Hami Gündoğdu[2], Mohammed A. Abdoon[3], Elmhadi Afif[4], Yousif M. Modawy[5] and Carlo Cattani[6]

[1]Department of Mathematics, Laboratory of Fundamental and Applied Mathematics of Oran (LMFAO), University of Oran 1 Ahmed Ben Bella, Oran, Algeria.
e-mail[1]: kadri.ilhem@univ-oran1.dz
[2]Department of Mathematics, Faculty of Science, Sakarya University, Sakarya, Turkey.
e-mail[2]: hamigundogdu@sakarya.edu.tr
[3,4]Department of Basic Sciences, Common First Year Deanship, King Saud University, Riyadh 12373, Saudi Arabia.
e-mai[3]: mabdoon.c@ksu.edu.sa, e-mail[4]: aahmad5.c@ksu.edu.sa
[5]Department of Mathematics, Al-Baha University, Al-Aqiq, Saudi Arabia.
e-mail[5]: yelmahy@bu.edu.sa
[6] Engineering School, University of Tuscia, Viterbo, Italy.
e-mail[6]: cattani@unitus.it

Abstract

This study explores the application of fractional operators to model diffusion, dispersion, dissipation, and reaction processes. Specifically, it examines the initial value problem using Caputo and conformable operators, employing the Laplace-Adomian decomposition method to derive approximate solutions. The solutions obtained are illustrated in 2D and 3D for specific values of fractional order, demonstrating their convergence. In addition, the absolute errors between the exact and approximate solutions are calculated and compared to the constructed problems. The advantages and limitations of each fractional operator are explored in terms of model accuracy, computational efficiency, and physical interpretability. This analysis reveals that conformable operator-based solutions demonstrate superior convergence rates and reduced error magnitudes compared to those obtained with the Caputo operator. In particular, the conformable solutions exhibit a more rapid convergence to the classical solution as the fractional order approaches one, suggesting a more accurate and computationally efficient representation of fractional-order dynamics. Conversely, the Caputo solutions display slower convergence and a greater deviation from the classical solution under similar conditions. These findings suggest that the conformable derivative provides a more precise and effective approximation to the classical solution, offering potential advantages for modeling fractional-order dynamics.

Keywords: *fractional Kdv-Burger's-Fisher equation, Caputo operator, Conformable operator, Laplace Adomian decomposition method.*

MSC Classification 2020*:26A33, 35R11, 35K57, 35A25, 65L70*

Received 28 July 2025; Accepted 26 October 2025

1 Introduction

Fractional partial differential equations (FPDEs) play a crucial role in various fields, including physics, biology, engineering, fluid mechanics, and viscoelasticity [19, 36]. Since most FPDEs lack exact solutions, researchers often rely on approximate and numerical methods to address the solutions to these equations [21, 39, 40]. FPDEs extend traditional partial differential equations (PDEs) of integer order and find extensive applications across various scientific fields [4, 5, 7, 15, 30, 32]. Given their broad relevance, numerous operators have been introduced in the literature to address FPDEs [33, 41].

Many phenomena described by integer-order PDEs are challenging to capture effectively, which underscores the importance of studying FPDEs [20, 31]. Recently, researchers have attracted significant interest in these kinds of equations due to their extensive applications in various scientific and engineering fields. To explore the mechanisms governed by FPDEs, we focused on the time-fractional KdV-Burgers-Fisher type equation. This nonlinear equation encompasses the mechanisms of reaction, dispersion, and dissipation, integrating the diffusion properties of the Burgers and Fisher equations along with their reaction dynamics.

For clarity, we briefly recall these physical mechanisms: diffusion represents nonlinear transport (e.g., of heat or mass), dissipation corresponds to energy loss, dispersion quantifies the spreading of energy, and the reaction term typically models population dynamics leading toward equilibrium. These combined effects are elegantly captured by the KBF equation, introduced by Kocak [25] in the following form:

$$u_t + Kuu_x - \mu u_{xx} + Yu_{xxx} = gu(1-u) \tag{1}$$

which characterizes the dynamics of the desired function $\mathrm{u}(\mathrm{x},\mathrm{t})$ depending on time and space. The coefficients K, μ, Y, and g represent the diffusion, dissipation, dispersion, and reaction terms, respectively. The Eq. (1) includes many types of significant equations depending on the mentioned coefficients. For $\mu = g = 0$, it becomes the well-known KdV equation. In the case of $g = 0$, it becomes the KdV-Burger's equation. Taking $Y = g = 0$ in Eq. (1) converts it into Burger's equation. When $Y = 0$, we get the Burgers-Fisher equation. For $K = Y = 0$, the Fisher equation is acquired. If $K = \mu = 0$, then the Eq. (1) changes to the dispersive-Fisher equation.

Although these classical models have been widely studied [8, 12, 16, 37], investigations of the fractional form of the KBF equation remain limited. Few papers have looked at this equation since it has recently been proposed. In particular, the literature lacks comprehensive studies that analyze approximate solutions of its fractional variants. This gap motivates the present study, which develops an analytical framework using the Laplace Adomian Decomposition Method (LADM) to treat both Caputo and conformable fractional formulations.

This paper addresses the two types of time-fractional initial value problems for the KBF equation, defined as follows:

$$\ {}_{C}D_t^{\gamma}u + Kuu_x - \mu u_{xx} + Yu_{xxx} = R(u), \tag{2}$$

and

$$\ {}_{cf}D_t^{\gamma}u + Kuu_x - \mu u_{xx} + Yu_{xxx} = R(u), \tag{3}$$

subject to the initial condition;

$$u(x,0) = h(x). \tag{4}$$

where $R(u) = gu(1-u)$ is a logistic reaction function. In (2) and (3), ${}_C D_t^{\gamma}$ and ${}_{cf} D_t^{\gamma}$ denote the Caputo's and conformable operators, respectively. Hence, these equations characterize the time-fractional dispersion, dissipation, and diffusion model in nonlinear wave propagation with a logistic reaction term.

A key focus in the study of FPDEs is the development of exact and approximate solutions. Many techniques have been devised to obtain accurate numerical and exact solutions, with various methods applied to different types of equations. Exact and numerical solutions for non-linear FPDEs have been obtained using a range of mathematical techniques that have been developed and studied. Notable examples include the first-integral method [13], the sub-equation method [29], the fractional reduced differential transformation method [1], the q-homotopy analysis transform method [28], the Elzaki homotopy perturbation method [35], the Yang transform decomposition method [38], the natural transform decomposition method [10], the variational iteration transform method [6], the iteration method via decomposition technique [34], the Laplace Adomian decomposition method (LADM) [14, 17, 23].

One of the most powerful methods for solving FPDEs is the LADM. This approach offers several remarkable advantages, including rapid convergence to exact solutions after a finite number of iterations and exceptional stability against discretization and perturbation challenges. Additionally, the LADM simplifies the treatment of nonlinearities through the use of Adomian polynomials, which are particularly effective in managing complex terms. In this study, the LADM is employed to derive approximate solutions for the time-fractional KBF equation. To our knowledge, the initial value problems (2) and (3) with (4) have not been explored with the LADM for approximate solutions. In addition, we provide a detailed convergence and error analysis of the method. The findings not only offer a fresh perspective on the solution behavior but also contribute novel insights to the broader body of research on fractional-order dynamics. This work highlights the utility of LADM as a versatile and robust tool for addressing a wide range of FPDEs, with implications across numerous scientific and engineering disciplines.

This paper is organized as follows: Section 2 presents key information about Caputo and conformable derivatives, along with their properties. In Section 3, the LADM is explored in detail for FPDEs, focusing on both the Caputo and conformable derivatives. Section 4 discusses the application of LADM to obtain approximate solutions to the time-fractional KBF equation in both the Caputo and conformable senses. Section 5 provides a convergence and error analysis for the method. Finally, Section 6 concludes with a summary of the main findings.

2 Preliminaries and Notations

This section is dedicated to the basic definitions, properties, and notation related to fractional operators that are required throughout the paper. Both Caputo and conformable fractional derivatives are considered, since they describe distinct memory effects and lead to different dynamical behaviors in the fractional KBF equation. For more information on the mentioned fractional operators, see [18, 24, 26, 27].

2.1 Caputo's Fractional Operator

The well-known γ-th order Caputo's fractional derivative of a differentiable function $f(t)$ is defined by

$$\square_C D_t^{\gamma} f(t) = \frac{1}{\Gamma(n-\gamma)} \int_0^t \frac{f^{(n)}(s)}{(t-s)^{\gamma+1-n}}\, ds, \quad n-1 < \gamma \leq n, \tag{5}$$

where $\square_C D_t^{r}$ represents Caputo's fractional operator and $\Gamma(t)$ is the gamma function given by

$$\Gamma(t) = \int_0^{\infty} e^{-s} s^{t-1}\, ds. \tag{6}$$

For $0 < \gamma \leq 1$, the Caputo's fractional derivative turns into

$$\square_C D_t^{\gamma} f(t) = \frac{1}{\Gamma(1-\gamma)} \int_0^t \frac{f'(s)}{(t-s)^{\gamma}}\, ds, \quad 0 < \gamma \leq 1. \tag{7}$$

The Caputo definition is particularly suitable for initial value problems, since it allows the use of standard physical initial conditions in terms of integer-order derivatives (e.g., $u(x,0) = h(x)$). Some advantageous properties of Caputo's fractional derivative are given in the following:

$$\square_C D_t^{\gamma} t^m = \frac{\Gamma(1+m)}{\Gamma(1+m-\gamma)} t^{(m-\gamma)}, \tag{8}$$

$$\square_C D_t^{\gamma}\big(cf(t)\big) = cD_t^{\gamma}\big(f(t)\big), \tag{9}$$

$$\square_C D_t^{\gamma}(c) = 0, \tag{10}$$

$$\square_C D_t^{\gamma}\big(af(t) + cg(t)\big) = aD_t^{\gamma}\big(f(t)\big) + cD_t^{\gamma}\big(g(t)\big), \tag{11}$$

where a and c are arbitrary constants.

2.2 Conformable Fractional Operator

Let $\boldsymbol{f}: [\mathbf{0}, \infty[\rightarrow \boldsymbol{R}$ be a function.

1. The "conformable derivative" of $\boldsymbol{f}$ of order $\boldsymbol{\gamma}$ is defined by

$$\square_{cf}\boldsymbol{D}_{\boldsymbol{\gamma}}(\boldsymbol{f})(\boldsymbol{t}) = \lim_{\boldsymbol{\varepsilon}\to\mathbf{0}} \frac{\boldsymbol{f}(\boldsymbol{t} + \boldsymbol{\varepsilon t}^{\mathbf{1}-\boldsymbol{\gamma}}) - \boldsymbol{f}(\boldsymbol{t})}{\boldsymbol{\varepsilon}}, \ \boldsymbol{for\ all}\ \boldsymbol{t} > \mathbf{0},\ \boldsymbol{\gamma} \in [\mathbf{0}, \mathbf{1}],$$

where $\square_{cf} D_{\gamma}$ represents a conformable fractional operator.

2. f is considered γ-differentiable if γ-th order fractional derivative of f in a conformable sense exists.
3. If f is γ-differentiable in some $]0, a[$, $a > 0$ and

$$\lim_{t\to 0^+} f^{(\gamma)}(t),$$

exists, then we define

$$f^{(\gamma)}(0) = \lim_{t\to 0^+} f^{(\gamma)}(t).$$

Unlike the Caputo operator, the conformable derivative is local and better suited for problems focusing on short-term memory or smooth transitions, making it a useful comparison framework for our study. We give some important properties that satisfy the conformable derivative:

- $_{cf}^{\square}D_{\gamma}(af+bg) = a_{cf}D_{\gamma}(f) + b_{cf}D_{\gamma}(g),\ for\ all\ a,b \in R.$
- $_{cf}^{\square}D_{\gamma}(t^{p}) = pt^{p-\gamma},\ for\ all\ p \in R.$
- $_{cf}^{\square}D_{\gamma}(\lambda) = 0, for\ all\ constant\ functions\ f \equiv \lambda.$
- $_{cf}^{\square}D_{\gamma}(fg) = f_{cf}D_{\gamma}(g) + g_{cf}D_{\gamma}(f).$
- $_{cf}^{\square}D_{\gamma}\left(\frac{f}{g}\right) = \frac{g_{cf}D_{\gamma}(f) - f_{cf}D_{\gamma}(g)}{g^{2}}.$

2.3 Laplace Transform of Fractional Derivatives

The Laplace transform plays a central role in the Laplace-Adomian decomposition method (LADM). For the Caputo derivative:

$$\mathcal{L}\{{}^{C}D_{t}^{\gamma}f(t)\}(s) = s^{\gamma}F(s) - s^{\gamma-1}f(0), \tag{12}$$

while for the conformable derivative:

$$\mathcal{L}\{{}^{cf}D_{t}^{\gamma}f(t)\}(s) = s^{\gamma}F(s) - s^{\gamma-1}f(0), \tag{13}$$

so, both operators yield similar Laplace-domain structures but correspond to different time-domain interpretations.

2.4 Boundary and Initial Conditions

In this study, we consider bounded spatial domains $\boldsymbol{x} \in [\boldsymbol{0}, \boldsymbol{L}]$ with Dirichlet boundary conditions

$$\boldsymbol{u(0,t) = u(L,t) = 0}, \tag{14}$$

and initial condition

$$\boldsymbol{u(x,0) = h(x)}, \tag{15}$$

which represent physically significant constraints for many diffusion–reaction–dispersion systems such as plasma waves, traffic flow, or fluid–structure interactions. These conditions ensure well-posedness and allow straightforward Laplace transformations in time.

3 Description of the Proposed Method Methodology

In this section, we present the Laplace-Adomian decomposition method (LADM) to obtain approximate analytical solutions of the time-fractional Korteweg-de Vries-Burgers-Fisher (KBF) equations given by (2) and (3). The method combines the Laplace transform with the Adomian decomposition technique, providing a systematic framework to handle both linear and nonlinear operators. It also provides an overview of the method for FPDEs, highlighting the distinct applications of both Caputo and conformable

operators. The method offers a powerful approach for obtaining approximate solutions to complex FPDEs by decomposing the problem into a series of solvable components. We discuss how the decomposition method can be applied separately to each fractional operator, with a focus on their respective strengths and challenges. Additionally, the section outlines the key steps involved in implementing the Laplace-Adomian method, including the calculation of Adomian polynomials and the use of the Laplace transform to facilitate the solution process.

3.1 The LADM Approach for Caputo Fractional Model

In this section, we illustrate the application of the LADM method to FPDEs, with a particular focus on those involving the Caputo derivative. We walk through the key steps of the method, demonstrating how it effectively decomposes the problem into manageable components.

Let us take the time-fractional PDE given by

$$ {}_C D_t^{\gamma} u(x,t) = L\big(u(x,t)\big) + N\big(u(x,t)\big) + g(x,t) \quad n-1 < \gamma \le n, \tag{16} $$

with

$$ {}_C D_t^{r} u(x,0) = h(x), \quad r = 0,1,2,\dots,n-1, \tag{17} $$

$$ {}_C D_t^{n} u(x,0) = 0, \tag{18} $$

where $h(x)$ is a given function of x, L and N are the linear and nonlinear operators, respectively.

Note that the Laplace transform of ${}_C D_t^{\gamma} u(x,t)$ in Caputo's type is defined by

$$ \mathcal{L}\{{}_C D_t^{\gamma} u(t)\} = s^{\gamma}\mathcal{L}\{u(t)\} - \sum_{r=0}^{n-1} s^{\gamma-r-1}\, {}_C D_t^{r} u(0), \quad n-1 < \gamma \le n, \tag{19} $$

where s is the Laplace domain function [22].

The Laplace transform is first applied to both sides of (16). Then, it turns into

$$ \mathcal{L}\{{}_C D_t^{\gamma} u(x,t)\} = \mathcal{L}\big\{L\big(u(x,t)\big) + N\big(u(x,t)\big) + g(x,t)\big\}. \tag{20} $$

Taking the properties into account provides

$$ \mathcal{L}\{u(t)\} = \sum_{r=0}^{n-1} s^{-r-1}\, h_r(x) + \frac{1}{s^{\gamma}}\mathcal{L}\big\{L\big(u(x,t)\big) + N\big(u(x,t)\big) + g(x,t)\big\}. \tag{21} $$

In (21), applying the inverse operator of the Laplace transform to both sides gives

$$ u(x,t) = \sum_{r=0}^{n-1} \frac{t^r}{\Gamma(r+1)} h_r(x) + \mathcal{L}^{-1}\left\{\frac{1}{s^{\gamma}}\big(\mathcal{L}\{g(x,t)\}\big)\right\} $$

$$ + \mathcal{L}^{-1}\left\{\frac{1}{s^{\gamma}}\mathcal{L}\{L\big(u(x,t)\big) + N\big(u(x,t)\big)\}\right\}. \tag{22} $$

The LADM [3] proposes that solution $u(x,t)$ is represented by the following infinite series

$$u(x,t) = \sum_{i=0}^{\infty} u_i(x,t)\,, \tag{23}$$

where the functions $u_i(x,t),\ i = 0,1,2,\ldots$ are the components of the solution.

The nonlinear term $N\big(u(x,t)\big)$ is defined by

$$N\big(u(x,t)\big) = \sum_{i=0}^{\infty} A_i\ , \tag{24}$$

where A_i are the Adomian polynomials [2] given by

$$A_n = \frac{1}{n!}\frac{d^n}{d\alpha^n}\left[N\left(\sum_{n=0}^{\infty}\alpha^n u_n\right)\right], n = 0,1,2,\ldots \tag{25}$$

Putting (23) and (24) into equation (22) yields

$$\sum_{i=0}^{\infty} u_i(x,t) = \sum_{=0}^{n-1}\frac{t^r}{\Gamma(r+1)}h_r(x) + \mathcal{L}^{-1}\left\{\frac{1}{s^\gamma}\left(\mathcal{L}\{g(x,t)\}\right)\right\} + \sum_{i=0}^{\infty} cL^{-1}\left\{\frac{1}{s^\gamma}\mathcal{L}\{L\big(u_i(x,t)\big) + A_i\}\right\}. \tag{26}$$

From (26), the following relations are granted

$$u_0(x,t) = \sum_{r=0}^{n-1}\frac{t^r}{\Gamma(r+1)}h_r(x) + \mathcal{L}^{1}\left\{\frac{1}{s^\gamma}\left(\mathcal{L}\{g(x,t)\}\right)\right\}, \tag{27}$$

and

$$u_{i+1}(x,t) = \mathcal{L}^{-1}\left\{\frac{1}{s^\gamma}\mathcal{L}\{L\big(u_i(x,t)\big) + A_i\}\right\}, \quad i \geq 0. \tag{28}$$

(27) and (28) provide us with the components of the solution. Hence, the approximate analytical solution of the equation (16) subjected to the conditions (17) and (18) is obtained.

3.2 The LADM Approach for Conformable Operator Model

In this section, we illustrate the application of the LADM method to FPDEs, specifically those involving the conformable operator. We outline the steps of the method, demonstrating how it decomposes the problem into solvable parts. Furthermore, we emphasize the benefits of using the conformable derivative within this approach,

highlighting its efficiency and precision in providing accurate approximate solutions for various FPDEs.

We consider the following problem

$$\square_{cf}\boldsymbol{D_{\gamma}u(x,t)} = \boldsymbol{L\big(u(x,t)\big) + N\big(u(x,t)\big) + g(x,t)} \quad \boldsymbol{n-1 < \gamma \le n}, \tag{29}$$

subject to

$$\square_{cf}\boldsymbol{D_r u(x,0) = h(x)}, \quad \boldsymbol{r = 0,1,2,\dots,n-1}, \tag{30}$$

$$\square_{C}\boldsymbol{D_t^n u(x,0) = 0}. \tag{31}$$

It is worth noting that the Laplace transform of $\boldsymbol{D_t^{\gamma}u(x,t)}$ in conformable type is defined by

$$\boldsymbol{\mathcal{L}_{\gamma}\big\{\square_{cf}D_{\gamma}u(t)\big\}(s) = s\mathcal{F}_{\gamma}(s) - u(0)}, \quad \boldsymbol{s > 0}. \tag{32}$$

If the Laplace transform is applied to both sides of the Eq. (29) w.r.t $\boldsymbol{t}$, it turns into the following:

$$\boldsymbol{\mathcal{L}\{_{cf}D_t^{\gamma}u(x,t)\} = \mathcal{L}\big\{L\big(u(x,t)\big) + N\big(u(x,t)\big) + g(x,t)\big\}}. \tag{33}$$

Utilizing the properties given above provides

$$\boldsymbol{\mathcal{L}\{u(x,t)\} = \frac{1}{s}h_r(x) + \frac{1}{s}\mathcal{L}\big\{L\big(u(x,t)\big) + N\big(u(x,t)\big) + g(x,t)\big\}}. \tag{34}$$

The inverse Laplace operator is applied to both sides of the Eq. (34). Then, the following is granted:

$$\boldsymbol{u(x,t) = h_r(x) + \mathcal{L}^{-1}\left\{\frac{1}{s}(\mathcal{L}\{g(x,t)\})\right\} + \mathcal{L}^{-1}\left\{\frac{1}{s}\mathcal{L}\{L\big(u(x,t)\big) + N\big(u(x,t)\big)\}\right\}}. \tag{35}$$

By following the previous process technique, we get the following iterative algorithm

$$\boldsymbol{u_0(x,t) = h_r(x) + \mathcal{L}^{-1}\left\{\frac{1}{s}(\mathcal{L}\{g(x,t)\})\right\}}, \tag{36}$$

and

$$\boldsymbol{u_{i+1}(x,t) = \mathcal{L}^{-1}\left\{\frac{1}{s}\mathcal{L}\{L\big(u_i(x,t)\big) + A_i\}\right\}}, \quad \boldsymbol{i \ge 0}, \tag{37}$$

where equations (36) and (37) provide us with the components of the solution. Thus, the approximate analytical solution of the equation (16) subjected to the conditions (30) and (31) is obtained. The resulting series converges rapidly under mild smoothness

conditions on $\boldsymbol{h(x)}$ and $\boldsymbol{N(u)}$. Dependence on the fractional order $\boldsymbol{\gamma}$ can be directly observed through the contribution of $\boldsymbol{s^{-\gamma}}$ terms in the Laplace domain.

Compared with other analytical techniques such as the homotopy analysis method, variational iteration method, or natural transform methods, the LADM offers several advantages:

- It avoids linearization, perturbation, or discretization, preserving the nonlinear character of the problem.
- Only a few iterations are required to obtain a rapidly convergent series solution.
- It accommodates different fractional operators (Caputo and conformable) in a unified Laplace-domain framework.
- Analytical insight into the impact of the fractional order γ on the solution can be directly obtained.

These properties make LADM particularly suitable for nonlinear fractional PDEs like the KBF equation.

4 Applications

In this section, we provide numerical examples to demonstrate the efficiency and accuracy of the Laplace Adomian Decomposition Method (LADM) for solving the time fractional KBF equations. Both Caputo and Conformable are considered to highlight the

effect of different fractional operators on the solution behavior.

4.1 Caputo Fractional KBF Equation

Consider the fractional KBF equation with Caputo derivative

$$ {}_{C}\boldsymbol{D}_{t}^{\boldsymbol{\gamma}}\boldsymbol{u} + \boldsymbol{u}\boldsymbol{u}_{\boldsymbol{x}} - \boldsymbol{u}_{\boldsymbol{xx}} - \boldsymbol{u}_{\boldsymbol{xxx}} = -\boldsymbol{u}(\mathbf{1} - \boldsymbol{u}), \tag{38} $$

with

$$ \boldsymbol{u}(\boldsymbol{x}, \mathbf{0}) = \boldsymbol{e}^{\boldsymbol{x}}, \tag{39} $$

where ${}_{C}\boldsymbol{D}_{t}^{\boldsymbol{\gamma}}$represents the Caputo fractional derivative with $\mathbf{0} < \boldsymbol{\gamma} \leq \mathbf{1}$. In the Eq. (16), $\boldsymbol{L(u)} = \boldsymbol{u}_{\boldsymbol{xx}} - \boldsymbol{u}_{\boldsymbol{xxx}} - \boldsymbol{u}$, $\boldsymbol{N(u)} = \boldsymbol{u^2} - \boldsymbol{u}\boldsymbol{u}_{\boldsymbol{x}}$, and $\boldsymbol{f(x,t)} = \mathbf{0}$ are taken. Pursuing the way outlined earlier (20)-(26) yields the following equalities:

$$ \boldsymbol{u_0(x,t)} = \boldsymbol{e}^{\boldsymbol{x}}, \tag{40} $$

$$ \boldsymbol{u_{i+1}(x,t)} = \boldsymbol{\mathcal{L}^{-1}}\left\{\frac{\mathbf{1}}{\boldsymbol{s^{\gamma}}}\boldsymbol{\mathcal{L}}\{\boldsymbol{L(u_i(x,t))} + \boldsymbol{N(u_i(x,t))}\}\right\}, \boldsymbol{i} \geq \mathbf{1} \tag{41} $$

where $\boldsymbol{L(u_i)} = \boldsymbol{u_{i_{xx}}} - \boldsymbol{u_{i_{xxx}}} - \boldsymbol{u_i}$ and $\boldsymbol{N(u_i)} = \boldsymbol{A_i} + \boldsymbol{B_i}$, where $\boldsymbol{A_i}$ and $\boldsymbol{B_i}$ are the Adomian polynomials for $\boldsymbol{u_i^2}$ and $\boldsymbol{u_i u_{i_x}}$, respectively.

Eq. (41) provides us with the components as follows by (42):

$$\boldsymbol{u_1(x,t) = \mathcal{L}^{-1}\left\{\frac{1}{s^\gamma}\mathcal{L}\{L(u_0(x,t)) + N(u_0(x,t)\}\right\} = e^x \frac{t^\gamma}{\Gamma(\gamma+1)},}$$

$$\boldsymbol{u_2(x,t) = \mathcal{L}^{-1}\left\{\frac{1}{s^\gamma}\mathcal{L}\{L(u_1(x,t)) + N(u_1(x,t)\}\right\} = e^x \frac{t^{2\gamma}}{\Gamma(2\gamma+1)},}$$

$$\boldsymbol{u_3(x,t) = \mathcal{L}^{-1}\left\{\frac{1}{s^\gamma}\mathcal{L}\{L(u_2(x,t)) + N(u_2(x,t)\}\right\} = e^x \frac{t^{3\gamma}}{\Gamma(3\gamma+1)},}$$

$$\vdots$$

The partial sum $\boldsymbol{u_N(x,t) = \sum_{n=0}^{N} u_n(x,t)}$ provides an accurate approximation for the solution. Putting the components into (23) gives the desired solution.

$$\boldsymbol{u(x,t) = u_0 + u_1 + u_2 + u_3 + \cdots,} \tag{43}$$

$$\boldsymbol{u(x,t) = e^x\left(1 + \frac{t^\gamma}{\Gamma(\gamma+1)} + \frac{t^{2\gamma}}{\Gamma(2\gamma+1)} + \frac{t^{3\gamma}}{\Gamma(3\gamma+1)} + \cdots\right).} \tag{44}$$

The solution (43) can be written in a closed form

$$\boldsymbol{u(x,t) = e^x \sum_{n=0}^{\infty} \frac{t^{n\gamma}}{\Gamma(n\gamma+1)}.} \tag{45}$$

Putting $\boldsymbol{\gamma = 1}$ in (45) yields the exact solution

$$\boldsymbol{u(x,t) = e^{x+t}.} \tag{46}$$

4.2 Conformable Fractional KBF Equation

Consider the same problem but with the conformable derivative $\boldsymbol{{}^{cf}D_t^\gamma}$. The LADM procedure follows analogously, with

$$\boldsymbol{{}_{cf}D_t^\gamma u + uu_x - u_{xx} - u_{xxx} = -u(1-u),} \tag{47}$$

with

$$u(x,0) = e^x, \tag{48}$$

where $0 < \gamma \leq 1$.

In a similar manner, we obtain

$$u_0(x,t) = e^x, \tag{49}$$

and

$$\boldsymbol{u_1(x,t) = \mathcal{L}^{-1}\left\{\frac{1}{s^\gamma}\mathcal{L}\{L(u_0(x,t)) + N(u_0(x,t)\}\right\} = e^x\frac{t^\gamma}{\gamma}}\,, \tag{50}$$

$$\boldsymbol{u_2(x,t) = \mathcal{L}^{-1}\left\{\frac{1}{s^\gamma}\mathcal{L}\{L(u_1(x,t)) + N(u_1(x,t)\}\right\} = e^x\frac{t^{2\gamma}}{2!\,\gamma^2}}\,, \tag{51}$$

$$\boldsymbol{u_3(x,t) = \mathcal{L}^{-1}\left\{\frac{1}{s^\gamma}\mathcal{L}\{L(u_2(x,t)) + N(u_2(x,t)\}\right\} = e^x\frac{t^{3\gamma}}{3!\,\gamma^3}}\,, \tag{52}$$

and so on.

Putting the components into (23) gives the desired solution

$$u(x,t) = u_0(x,t) + u_1(x,t) + u_2(x,t) + u_3(x,t) + \cdots,$$

so,

$$u(x,t) = e^x\left[1 + \frac{t^\gamma}{\gamma} + \frac{t^{2\gamma}}{2!\,\gamma^2} + \frac{t^{3\gamma}}{3!\,\gamma^3} + \cdots\right] = e^x e^{\frac{t^\gamma}{\gamma}} = e^{x+\frac{t^\gamma}{\gamma}}, \tag{53}$$

For $\gamma = 1$, equation (42) grants the exact solution

$$u(x,t) = e^{x+t}. \tag{54}$$

Numerical computations show that:

- The LADM series converges rapidly for both Caputo and conformable derivatives.
- The fractional order γ significantly influences the amplitude and dispersion of the solution.
- For the conformable derivative, the local nature of the operator produces slightly smoother profiles compared with the Caputo derivative.
- Dirichlet boundary conditions are preserved at each iteration, ensuring physically meaningful solutions.

These results validate the effectiveness and flexibility of LADM for solving nonlinear time-fractional PDEs in both Caputo and conformable senses. Furthermore, the LADM requires no mesh generation, linearization, or iterative solvers; thus, its computational complexity grows linearly with the number of iterations. In symbolic implementations (e.g., Maple, Mathematica), all operations are analytical, leading to very low runtime even for complex nonlinearities. Compared to finite difference or homotopy-based methods, the LADM is both computationally efficient and memory-light, while retaining analytical interpretability.

4.3 Solution Accuracy Variations Across Varied Methodologies

The approximate solutions of the time-fractional KBF equation involving Caputo and conformable derivatives are analyzed numerically and graphically for different values of γ. The solutions are examined to observe their behavior and convergence patterns as the fractional order varies. Graphical representations illustrate the distinct characteristics of each approach, providing insights into the solution dynamics for various values of γ.

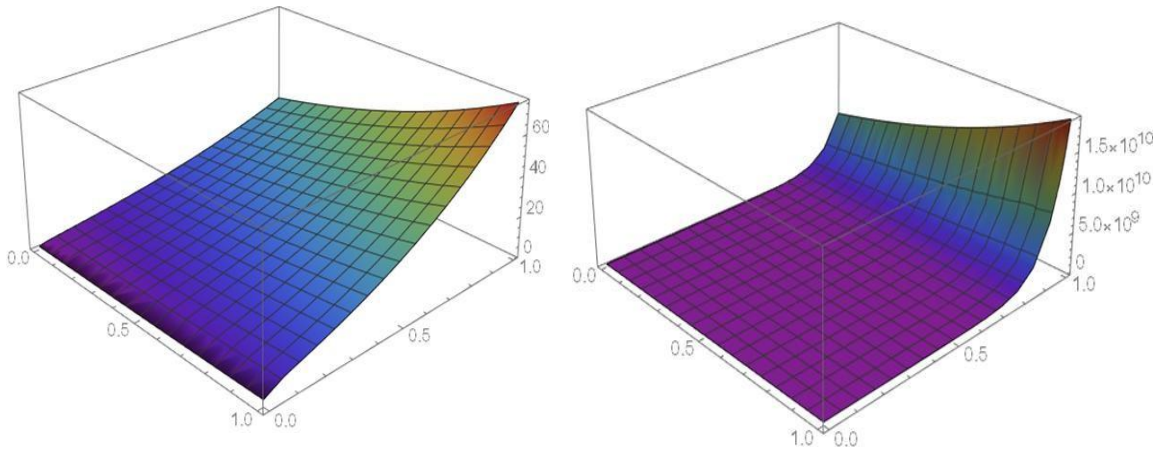

(a) Caputo's sense for $\gamma = 0.25$. (b) Conformable sense for $\gamma = 0.25$.

Fig. 1: Surface plots of the approximate solutions for $\gamma = 0.25$ in Caputo and conformable senses, respectively.

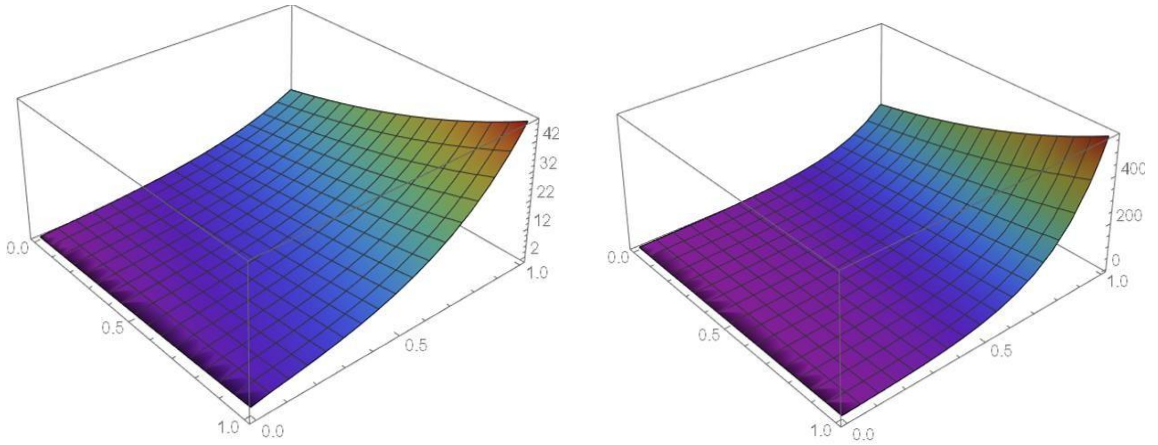

(a) Caputo's sense for $\gamma = 0.5$. (b) Conformable sense for $\gamma = 0.5$.

Fig. 2: Surface plots of the approximate solutions for $\gamma = 0.5$ in Caputo and conformable senses, respectively.

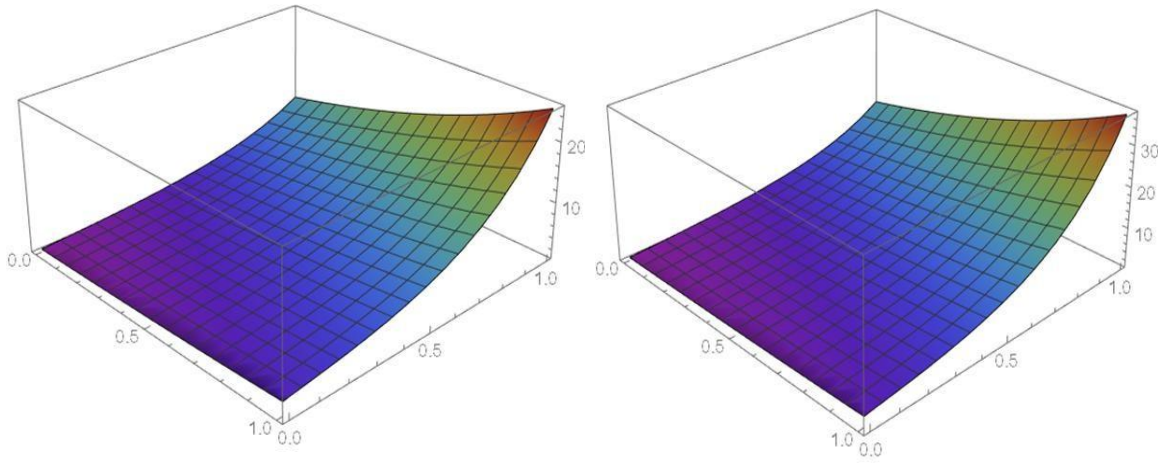

(a) Caputo's sense for $\gamma = 0.75$. (b) Conformable sense for $\gamma = 0.75$.

Fig. 3: Surface plots of the approximate solutions for $\gamma = 0.75$ in Caputo and conformable senses, respectively.

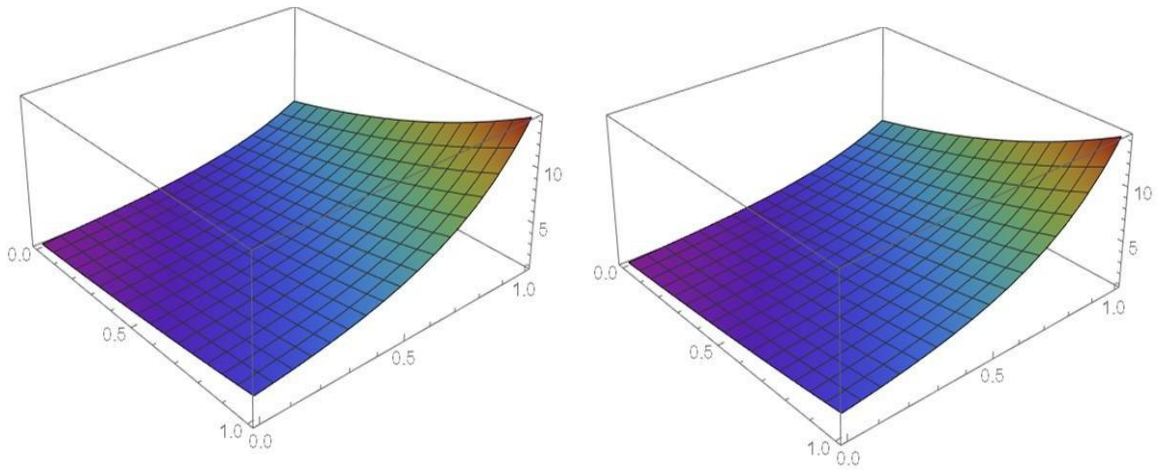

(a) Caputo's sense for $\gamma = 1$. (b) Conformable sense for $\gamma = 1$.

Fig. 4: Surface plots of the approximate solutions for $\gamma = 1$ in Caputo and conformable senses, respectively.

The surface plots illustrating the approximate solutions obtained using Caputo's and conformable derivatives are presented in Figs. (1) through (4). These figures demonstrate the behavior of the solutions as a function of the parameter γ. Although the plots exhibit a similar overall shape at each step, subtle differences in the solution values are evident, highlighting the nuanced variations between the two methods. The contour plots, which illustrate the corresponding solutions, are likewise presented. The distinction between them becomes strikingly evident, as demonstrated in (6) and (7).

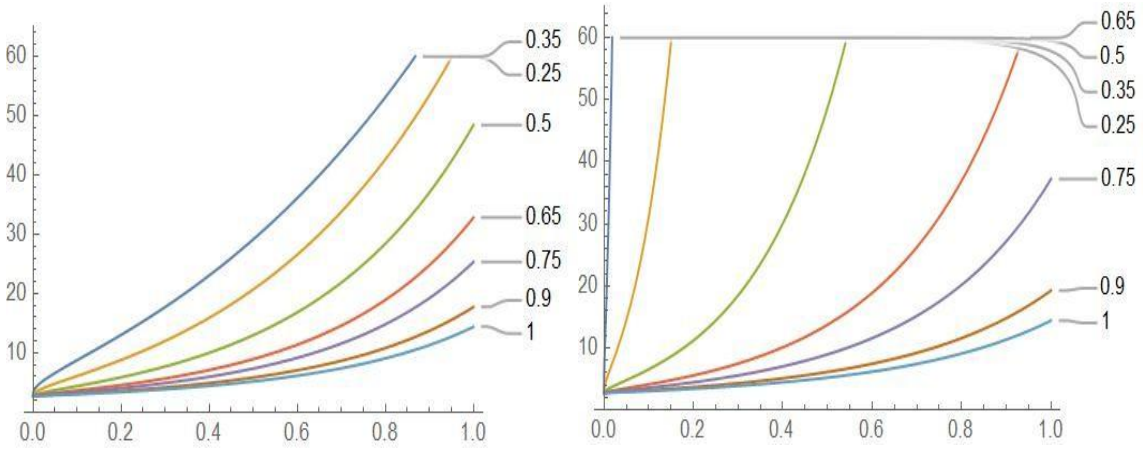

(a) Approximations in Caputo's sense as $\gamma \to 1$.

(b) Approximations in Caputo's sense as $\gamma \to 1$.

Fig. 5: 2D plots of the approximate solutions for different values of γ in Caputo and conformable senses.

Fig. (5) illustrates that, as $\gamma \to 1$, the solutions of the problem considered in the conformable sense converge to the classical solution more rapidly. The error between the conformable solutions and the classical solution decreases at a faster rate, indicating more efficient convergence. In contrast, the solutions in the Caputo sense exhibit slower convergence, with a larger deviation from the classical solution even as γ approaches 1. This behavior highlights that the conformable derivative provides a more accurate and effective approximation to the classical solution in the limit. These results suggest that the conformable derivative may offer enhanced performance in modeling fractional-order dynamics, especially for problems where a more precise approximation to the classical solution is required. Additionally, the faster convergence observed in the conformable sense may lead to computational advantages in certain applications.

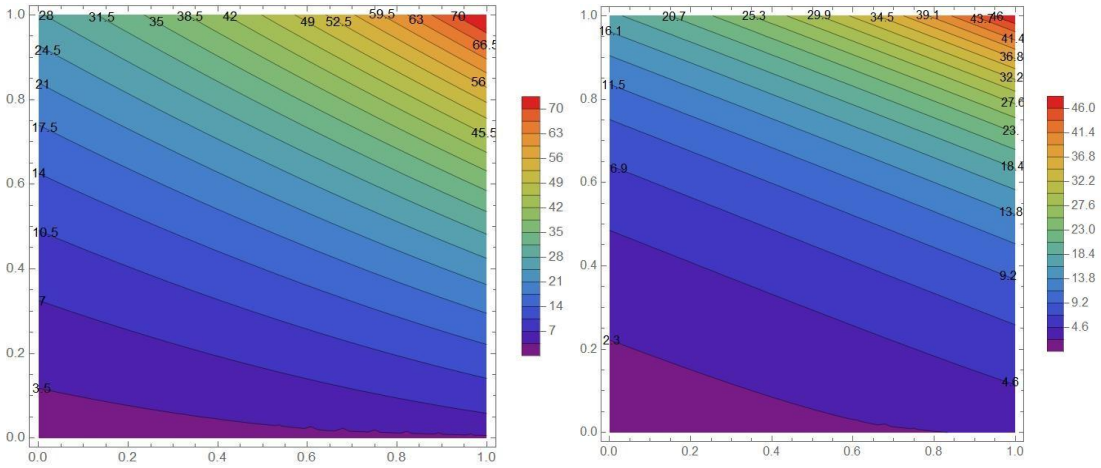

(a) $\gamma = 0.25$.

(b) $\gamma = 0.5$.

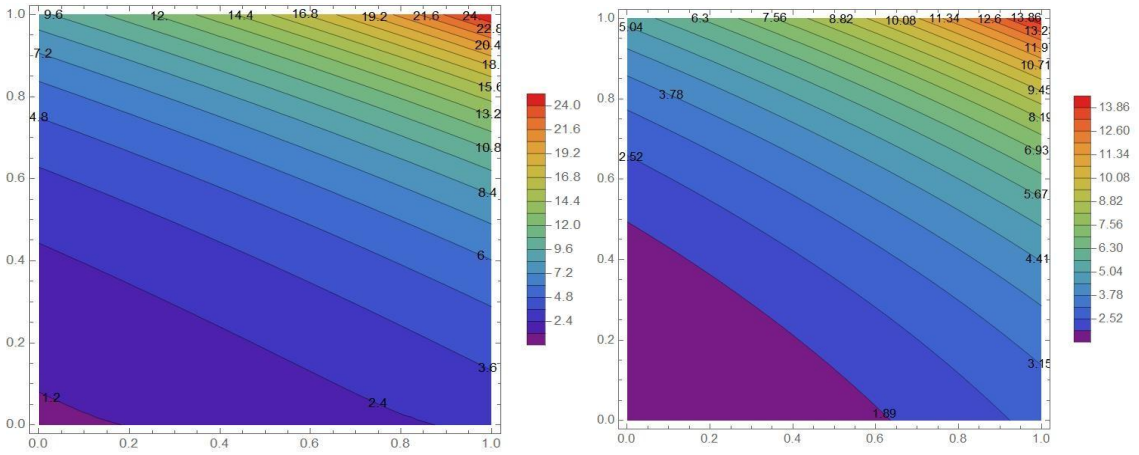

(c) $\gamma = 0.75$. (d) $\gamma = 1$.

Fig. 6: Contour plots of the approximate solutions for different values of γ in Caputo's sense.

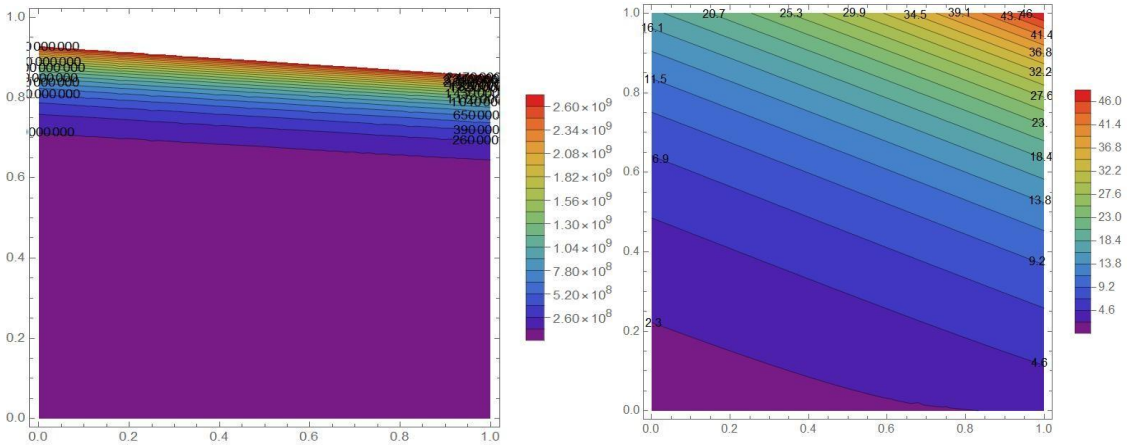

(a) $\gamma = 0.25$. (b) $\gamma = 0.5$.

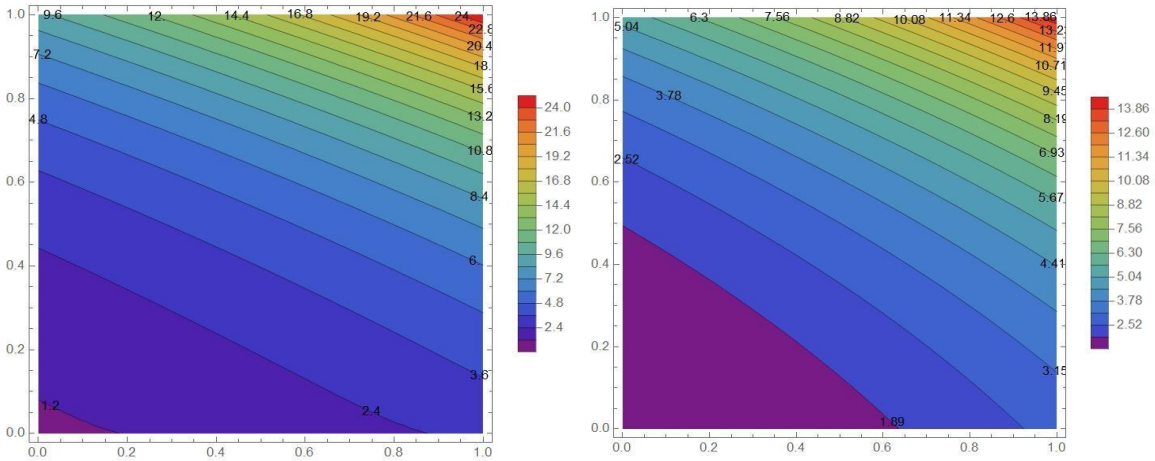

(c) $\gamma = 0.75$. (d) $\gamma = 1$.

Fig. 7: Contour plots of the approximate solutions for different values of γ in conformable sense.

5 Analysis of Error Propagation and Convergence

We present the sufficient conditions for the convergence and provide an error analysis for the method described above. It is proposed that the solution is of the following form

$$u(x,t) = \sum_{i=0}^{\infty} u_i(x,t)\,. \tag{55}$$

Theorem 5.1

If there exists $0 < M < 1$ s.t

$$\big||u_{i+1}(x,t)|\big| \le H\big||u_i(x,t)|\big|, \quad \forall i \ge i_0, \tag{56}$$

for some i_0, then the solution (55) is convergent.

Proof:

The Banach space $(C([I]), ||.||)$ of all continuous functions $f(x,t)$ on the interval I with the usual norm $\big||f(x,t)|\big| = \max_{(x,t)\in I}|f(x,t)|$ is considered.

Let S_n be a sequence of the following sum

$$S_n = u_0(x,t) + u_1(x,t) + \cdots + u_n(x,t). \tag{57}$$

It will be shown that S_n is a Cauchy sequence in $(C([I]), ||.||)$. Indeed,

$$\big||S_{n+1} - S_n|\big| = \big||u_{n+1}|\big| \le H\big||u_n|\big| \le \cdots \le H^{n-i_0+1}\Big||u_{i_0}|\Big|. \tag{58}$$

Then, we have

$$\big||S_n - S_m|\big| = \left|\left|\sum_{k=m}^{n-1}(S_{k+1} - S_k)\right|\right| \le \sum_{k=m}^{n-1}\big|\big|(S_{k+1} - S_k)|\big|, \tag{59}$$

$$\le \sum_{k=m}^{n-1}\Big||u_{i_0}|\Big| = \frac{1-H^{n-m}}{1-H}H^{m-i_0+1}\Big||u_{i_0}|\Big|, \tag{60}$$

for every $n, m \in N$ and $n \ge m > i_0$.

As $0 < H < 1$, we reach the following

$$lim_{n,m\to\infty}\big||S_n - S_m|\big| = 0. \tag{61}$$

The following theorem provides us with the estimate for maximum absolute truncated error.

Theorem 5.2

Let $\sum_{i=0}^{m} u_i(x,t)$ an approximate solution. Then the maximum absolute error between the approximate and exact solution is computed as

$$\left|\left|u(x,t) - \sum_{i=0}^{m} u_i(x,t)\right|\right| \le \frac{H^{m+1}}{1-H}\big||u_0(x,t)|\big|. \tag{62}$$

Proof:

$$\left\| u(x,t) - \sum_{i=0}^{m} u_i(x,t) \right\| = \left\| \sum_{i=m+1}^{\infty} u_i(x,t) \right\| \leq \sum_{i=m+1}^{\infty} \left\| u_i(x,t) \right\|, \tag{63}$$

$$\leq \sum_{i=m+1}^{\infty} H^i \left\| u_0(x,t) \right\| \leq \frac{H^{m+1}}{1-H} \left\| u_0(x,t) \right\|. \tag{64}$$

It concludes the proof.

In addition to the graphical comparison, the solutions are also compared numerically for $t = 0.01$ and specific values of γ.

Absolute errors of the Caputo-type time-fractional KBF (38) subject to the (39) are given in the following table.

Table 1: Maximum absolute error for the Eq. (34) in Caputo sense with $t = 0.01$

x/γ	0.45	0.75	0.95
1	9.20775×10^{-3}	2.02589×10^{-4}	5.18474×10^{-6}
2	1.12464×10^{-2}	2.47444×10^{-4}	6.33265×10^{-6}
3	1.37364×10^{-2}	3.02229×10^{-4}	7.73472×10^{-6}
4	1.67776×10^{-2}	3.69143×10^{-4}	9.44721×10^{-6}
5	2.04922×10^{-2}	4.50872×10^{-4}	1.15388×10^{-5}

For the conformable time-fractional KBF equation KBF (43) subject to the (44), we have the following absolute errors.

Table 2: Maximum absolute error for the Eq. (43) in conformable sense with $t = 0.01$

x/γ	0.45	0.75	0.95
1	3.30033×10^{-4}	1.62209×10^{-7}	1.57364×10^{-9}
2	4.03104×10^{-4}	1.98123×10^{-7}	1.92205×10^{-9}
3	4.92352×10^{-4}	2.41988×10^{-7}	2.34759×10^{-9}
4	6.01361×10^{-4}	2.95564×10^{-7}	2.86736×10^{-9}
5	7.34503×10^{-4}	3.61003×10^{-7}	3.50219×10^{-9}

Analyzing the results represented in Tabs. (1) and (2) illustrates that the approximate solutions obtained for the KBF equation in the conformable sense are more precise than the ones found for the Caputo-type. Besides, the quantitative analysis of the error between the solutions obtained using the conformable and Caputo fractional operator and the classical solution reveals a marked difference in their performance. For large values of γ, the conformable derivative method consistently achieves a sig- nificantly smaller error compared to the Caputo sense. This discrepancy becomes even more

pronounced as γ approaches 1. In this limiting case, the solutions in the con- formable sense converge more closely to the classical solution, demonstrating a more accurate and precise approximation. In contrast, the solutions derived from the Caputo sense exhibit a larger error, underscoring the superior efficiency and precision of the conformable operator in approximating the classical solution as $\gamma \to 1$.

6 Conclusion

This study examines the time-fractional KBF equation, a sophisticated model that encompasses diffusion, dispersion, dissipation, and logistic reaction processes, using both Caputo and conformable fractional derivatives. The solutions obtained are visually displayed in 3D and also presented in 2D for various values of γ. Visualizations in 2D and 3D demonstrate the convergence of approximate solutions to the exact solution as the fractional order $\gamma \to 1$. As shown in graphical representations and tabulated absolute error data, the approximation based on the conformable derivative yields superior accuracy compared to the Caputo derivative. This advantage stems from the conformable derivative's straightforward definition, simplifying its application and mitigating the computational complexities inherent in traditional fractional calculus. Furthermore, the conformable derivative aligns with key properties of classical derivatives, such as product, quotient, and chain rules, which are not fully satisfied by the Caputo derivative, enhancing its applicability across diverse fields. Approximate solutions for the KBF equation were obtained using the Laplace-Adomian Decomposition Method (LADM), a direct and efficient approach to solving fractional partial differential equations (FPDE). The LADM's ability to easily handle different fractional derivatives makes it an ideal tool for addressing a wide range of FPDEs in science and engineering. This comparative study underscores the efficacy of fractional operators, specifically Caputo and conformable derivatives, in modeling diffusion, dispersion, dissipation, and reaction processes. Our findings demonstrate their potential to capture nonlocal and memory effects, offering a more accurate and flexible approach compared to integer-order models.

The fractional order parameter allows for precise model tuning to match experimental data and physical insights. However, the optimal choice of the fractional operator depends on the system's specific characteristics. By advancing our understanding of fractional calculus and its applications, we can unlock new insights into complex systems and develop innovative solutions to real-world challenges.

Future research may focus on several extensions of the current framework: Incorporating multi-dimensional geometries and more complex boundary conditions (e.g., Neumann, mixed-type) to study anisotropic effects; Extending the method to stochastic or uncertain fractional models using random perturbations or noise terms; Conducting a rigorous stability and convergence analysis under variable-order fractional operators; Combining the LADM with Monte Carlo simulations or spectral techniques to quantify uncertainty and improve computational performance; Such developments will further establish the LADM as a powerful analytical-numerical hybrid tool for solving a wide range of nonlinear fractional physical and engineering systems.

Conflict of interest: On behalf of all authors, the corresponding author states that there is no conflict of interest.

ACKNOWLEDGEMENTS
We would like to express our sincere appreciation to the reviewers for their generous support and assistance in enhancing the quality of this work.

References

[1] Abuasad, S., Hashim, I., & Abdul Karim, S. A. (2019). Modified Fractional Reduced Differential Transform Method for the Solution of Multiterm Time-Fractional Diffusion Equations. *Advances in Mathematical Physics*, *2019*(1), 5703916.

[2] Adomian, G., & Rach, R. (1983). Inversion of nonlinear stochastic operators. *Journal of Mathematical Analysis and Applications*, *91*(1), 39-46.

[3] Adomian, G. (2013). *Solving frontier problems of physics: the decomposition method* (Vol. 60). Springer Science & Business Media.

[4] Ahmad, S., Ullah, A., Akg, A., & Baleanu, D. (2022). On solution of fractional model of human liver under hybrid fractional derivative. *Discontinuity, Nonlinearity, and Complexity*, *11*(01), 183-190.

[5] Akram, T., Abbas, M., & Ali, A. (2021). A numerical study on time fractional Fisher equation using an extended cubic B-spline approximation. *J. Math. Comput. Sci*, *22*(1), 85-96.

[6] Alderremy, A. A., Aly, S., Fayyaz, R., Khan, A., Shah, R., & Wyal, N. (2022). The Analysis of Fractional-Order Nonlinear Systems of Third Order KdV and Burgers Equations via a Novel Transform. *Complexity*, *2022*(1), 4935809.

[7] Alqahtani, R. T., Ahmad, S., & Akgül, A. (2021). Mathematical analysis of biodegradation model under nonlocal operator in Caputo sense. *Mathematics*, *9*(21), 2787.

[8] Ali, S., & Javid, A. (2023). EXPLICIT SOLUTIONS FOR THE CONFORMABLE REGULARIZED LONG WAVE BURGER'S EQUATION. *Journal of Applied Analysis & Computation*, *13*(1), 344-358.

[9] Atangana, A., & Baleanu, D. (2016). New fractional derivatives with nonlocal and non-singular kernel: theory and application to heat transfer model. *arXiv preprint arXiv:1602.03408*.

[10] Botmart, T., Agarwal, R. P., Naeem, M., Khan, A., & Shah, R. (2022). On the solution of fractional modified Boussinesq and approximate long wave equations with non-singular kernel operators. *AIMS Math*, *7*(7), 12483-12513.

[11] Caputo, M., & Fabrizio, M. (2015). A new definition of fractional derivative without singular kernel. *Progress in fractional differentiation & applications*, *1*(2), 73-85.

[12] Çelikkaya, İ., & Guzel, A. (2023). FOUR NUMERICAL SCHEMES FOR SOLUTION OF BURGERS'EQUATION VIA OPERATOR SPLITTING TRIGONOMETRIC CUBIC B-SPLINE COLLOCATION METHOD. *Journal of Applied Analysis and Computation*, *13*, 313-328.

[13] Feng, Z. (2002). The first-integral method to study the Burgers–Korteweg–de Vries equation. *Journal of Physics A: Mathematical and General*, *35*(2), 343.

[14] Gündoğdu, H., & Gözükızıl, Ö. F. (2017). Obtaining the solution of Benney-Luke Equation by Laplace and adomian decomposition methods. *Sakarya University Journal of Science*, *21*(6), 1524-1528.

[15] Gündoğdu, H., & Joshi, H. (2025). Numerical analysis of time-fractional cancer models with different types of net killing rate. *Mathematics*, *13*(3), 536.

[16] Foadian, S., Pourgholi, R., Tabasi, S. H., & Zeidabadi, H. (2020). Solving an inverse problem for a generalized time-delayed Burgers-fisher equation by haar wavelet method. *J. Appl. Anal. Comput*, *10*(2), 391-410.

[17] Gundogdu, H., & Gozukizil, O. F. (2022). On the approximate numerical solutions of fractional heat equation with heat source and heat loss. *Thermal Science*, *26*(5 Part A), 3773-3786.

[18] He, W., Rui, W., & Hong, X. (2024). An extensional conformable fractional derivative and its effects on solutions and dynamical properties of fractional partial differential equations. *Journal of Applied Analysis & Computation*, *14*(3), 1790-1819.

[19] Inc, M. (2008). The approximate and exact solutions of the space-and time-fractional Burger's equations with initial conditions by variational iteration method. *Journal of Mathematical Analysis and Applications*, *345*(1), 476-484.

[20] Kadri, I., Saadeh, R. S., AlMutairi, D. M., Dafaalla, M. E., Berir, M., & Abdoon, M. A. (2025). Analytical and Numerical Investigation of a Fractional Order 4D Chaotic System via Caputo Fractional Derivative. *European Journal of Pure and Applied Mathematics*, *18*(3), 6381-6381.

[21] Jafari, H., & Daftardar-Gejji, V. (2006). Solving linear and nonlinear fractional diffusion and wave equations by Adomian decomposition. *Applied Mathematics and Computation*, *180*(2), 488-497.

[22] Jarad, F., & Abdeljawad, T. (2020). Generalized fractional derivatives and Laplace transform.

[23] Ilhem, K., Al Horani, M., & Khalil, R. R. (2022). Solution of Non-linear Fractional Burger's Type Equations Using The Laplace Transform Decomposition Method. *Results in Nonlinear Analysis*, *5*(2), 131-150.

[24] Jia, H., Nie, Y., & Zhao, Y. (2025). General Conformable Fractional Double Laplace-Sumudu Transform and its Application. *J. Appl. Anal. Comput*, *15*, 9-20.

[25] Koçak, H. (2020). Traveling waves in nonlinear media with dispersion, dissipation, and reaction. *Chaos: An Interdisciplinary Journal of Nonlinear Science*, *30*(9).

[26] Mahdy, A. M. S. (2024). Numerical solution and optimal control for fractional tumor immune model. *J. Appl. Anal. Comput*, *14*(5), 3033-3045.

[27] Masti, I., Sayevand, K., & Jafari, H. (2024). On epidemiological transition model of the Ebola virus in fractional sense. *J. Appl. Anal. Comput.*, *14*(3), 1625-1647.

[28] Prakash, A., Veeresha, P., Prakasha, D. G., & Goyal, M. (2019). A new efficient technique for solving fractional coupled Navier–Stokes equations using q-homotopy analysis transform method. *Pramana*, *93*(1), 6.

[29] Rezazadeh, H., & Ziabarya, B. P. (2016). Sub-equation method for the conformable fractional generalized kuramoto sivashinsky equation. *Comput. Res. Prog. Appl. Sci. Eng*, *2*(3), 106-109.

[30] Roozbahani, M. M., Aminikhah, H., & Tahmasebi, M. (2018). Numerical solution of stochastic fractional pdes based on trigonometric wavelets. *UPB Sci. Bull. Ser. A Appl. Math. Phys*, *80*, 161-174.

[31] Kadri, I., Gundogdu, H., Modawy, Y. M., Imam, A., Helal, K. A., Elshamy, I., & Tahir, R. A. (2025). A Comparative Analysis of the Non-linear Time Fractional Whitham-Broer-Kaup Equations under Aboodh Decomposition Transform. *European Journal of Pure and Applied Mathematics*, *18*(3), 6626-6626.

[32] Saifullah, S., Ali, A., Irfan, M., & Shah, K. (2021). Time-Fractional Klein–Gordon Equation with Solitary/Shock Waves Solutions. *Mathematical Problems in Engineering*, *2021*(1), 6858592.

[33] Kadri, I., Al Horani, M., & Khalil, R. (2023). Solution of fractional Laplace type equation in conformable sense using fractional fourier series with separation of variables technique. *Results in Nonlinear Analysis*, *6*(2), 53-59.

[34] Shah, F. A., & Noor, M. A. (2017). Application of decomposition technique and efficient methods for the approximate solution of nonlinear equations. *Appl. Math. Phys.*, *79*(3), 171-180.

[35] Shah, N. A., El-Zahar, E. R., Akgül, A., Khan, A., & Kafle, J. (2022). Analysis of Fractional-Order Regularized Long-Wave Models via a Novel Transform. *Journal of Function Spaces*, *2022*(1), 2754507.

[36] Ahmed, A. I., Elbadri, M., Alotaibi, A. M., Ashmaig, M. A., Dafaalla, M. E., & Kadri, I. (2025). Chaos and Dynamic Behavior of the 4D Hyperchaotic Chen System via Variable-Order Fractional Derivatives. *Mathematics*, *13*(20), 3240.

[37] Wang, Z., Zhang, L., & Liu, H. (2020). LIE SYMMETRY ANALYSIS TO FISHER'S EQUATION WITH TIME FRACTIONAL ORDER. *Journal of Applied Analysis & Computation*, *10*(5), 2058-2067.

[38] Zidan, A. M., Khan, A., Shah, R., Alaoui, M. K., & Weera, W. (2022). Evaluation of time-fractional Fisher’s equations with the help of analytical methods. *Aims Math*, *7*(10), 18746-66.

[39] Batiha, I. M., Jebril, I. H., Zuriqat, M., Kanaan, H. S., & Momani, S. (2023). An efficient approach for solving one-dimensional fractional heat conduction equation. *Frontiers in Heat and Mass Transfer*, *21*(1), 487-504.

[40] Batiha, I. M., Jebril, I. H., Anakira, N., Al-Nana, A. A., Batyha, R., & Momani, S. (2024). Two-dimensional fractional wave equation via a new numerical approach. *International Journal of Innovative Computing, Information & Control*, *20*(4), 1045-1059.

[41] Bouchenak, A., Batiha, I. M., Aljazzazi, M., Jebril, I. H., Al-Horani, M., & Khalil, R. (2024). Atomic exact solution for some fractional partial differential equations in Banach spaces. *Partial Differential Equations in Applied Mathematics*, *9*, 100626.